

MOURA, D.S., PESTANA, C.J., MOFFAT, C.F., GKOLEMANI, N., HUI, J., IRVINE, J.T.S. and LAWTON, L.A. 2024. Aging microplastics enhances the adsorption of pharmaceuticals in freshwater. *Science of the total environment* [online], 912, article number 169467. Available from: <https://doi.org/10.1016/j.scitotenv.2023.169467>

Aging microplastics enhances the adsorption of pharmaceuticals in freshwater.

MOURA, D.S., PESTANA, C.J., MOFFAT, C.F., GKOLEMANI, N., HUI, J.,
IRVINE, J.T.S. and LAWTON, L.A.

2024



Aging microplastics enhances the adsorption of pharmaceuticals in freshwater

Diana S. Moura^{a,*}, Carlos J. Pestana^a, Colin F. Moffat^a, Nikoletta Gkoulemani^b, Jianing Hui^b, John T.S. Irvine^b, Linda A. Lawton^a

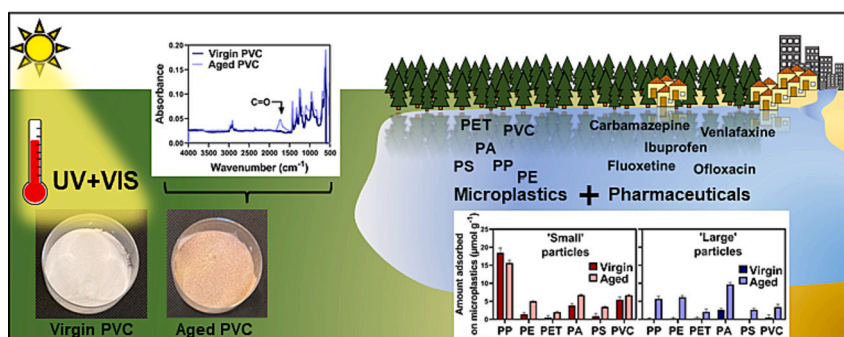
^a School of Pharmacy and Life Sciences, Robert Gordon University, Aberdeen AB10 7GJ, UK

^b School of Chemistry, University of St Andrews, North Haugh, St Andrews, Scotland KY16 9ST, UK

HIGHLIGHTS

- Five pharmaceuticals were brought into contact with six plastics sized $D_{50} < 35$ and 95–157 μm
- The particles were artificially aged to study how photo-oxidation affects adsorption of the selected pharmaceuticals
- Pharmaceuticals generally showed greater adsorption onto aged plastics than onto virgin plastics
- Of the five pharmaceuticals, fluoxetine showed greatest adsorption onto microplastics
- Polypropylene, polyamide, and polyvinylchloride exhibited the greatest adsorption of pharmaceuticals

GRAPHICAL ABSTRACT



ARTICLE INFO

Editor: Damià Barceló

Keywords:

Water pollution
Polymer
Weathering
Photo-oxidation
Carboxyl index

ABSTRACT

Plastic pollution is an increasing environmental concern. Pollutants such as microplastics (< 5 mm) and pharmaceuticals often co-exist in the aquatic environment. The current study aimed to elucidate the interaction of pharmaceuticals with microplastics and ascertain how the process of photo-oxidation of microplastics affected the adsorption of the pharmaceuticals. To this end, a mixture containing ibuprofen, carbamazepine, fluoxetine, venlafaxine and ofloxacin ($16 \mu\text{mol L}^{-1}$ each) was placed in contact with one of six either virgin or aged microplastic types. The virgin microplastics were acquired commercially and artificially aged in the laboratory. Polypropylene, polyethylene, polyethylene terephthalate, polyamide, polystyrene, and polyvinyl chloride microparticles at two sizes described as small ($D_{50} < 35 \mu\text{m}$) and large ($D_{50} 95\text{--}157 \mu\text{m}$) were evaluated. Results demonstrated that the study of virgin particles may underestimate the adsorption of micropollutants onto microplastics. For virgin particles, only small microparticles of polypropylene, polyethylene, polyvinyl chloride, and both sizes of polyamide adsorbed pharmaceuticals. Aging the microplastics increased significantly the adsorption of pharmaceuticals by microplastics. Fluoxetine adsorbed onto all aged microplastics, from 18 % (large polyethylene terephthalate) to 99 % (small polypropylene). The current investigation highlights the potential of microplastics to act as a vector for pharmaceuticals in freshwater, especially after aging.

* Corresponding author.

E-mail address: d.souza-moura1@rgu.ac.uk (D.S. Moura).

<https://doi.org/10.1016/j.scitotenv.2023.169467>

Received 6 October 2023; Received in revised form 7 December 2023; Accepted 16 December 2023

Available online 22 December 2023

0048-9697/© 2023 The Authors. Published by Elsevier B.V. This is an open access article under the CC BY license (<http://creativecommons.org/licenses/by/4.0/>).

1. Introduction

Contaminants are ubiquitous in aquatic environments. The pollutants found in water vary from plastic materials (Yao et al., 2020) to dissolved organic compounds, including pharmaceuticals (Kandie et al., 2020). When in the environment, plastics can fragment due to physical, chemical, and biological degradation (Napper and Thompson, 2019). Plastic particles smaller than 5 mm in all dimensions are commonly defined as microplastics (Thompson et al., 2009). Microparticles of polypropylene (PP), polyethylene (PE), polyethylene terephthalate (PET), polyamide (PA), polystyrene (PS), and polyvinyl chloride (PVC) are a significant presence in aquatic systems (Koelmans et al., 2019). According to the World Health Organisation (WHO), microplastic particle counts ranged from around 0 to 1000 particles per litre in freshwater studies while drinking water studies reported particle counts in individual samples from 0 to 10,000 particles per litre (WHO, 2019). The occurrence of specifically PP, PE, PET, PA, PS, and PVC in freshwater systems should be anticipated since those plastics represent approximately 80 % of the polymeric materials distributed annually (Plastics Europe, 2021). Due to the regular detection of microplastics in the aquatic environment, several studies have been published about the interaction of microplastics with co-occurring pollutants (Magadini et al., 2020; Pestana et al., 2021; Torres et al., 2021). In order to conduct adsorption experiments with microplastics, researchers have either acquired microplastics commercially (Moura et al., 2022) or produced them in the laboratory by grinding (Elizalde-velázquez et al., 2020; Pestana et al., 2021; Wu et al., 2016) or milling larger sized plastics (Xu et al., 2018). However, virgin microplastics may not be environmentally the most representative of the microplastics present in the environment. Plastics in the environment are exposed to solar radiation that can lead to thermal and photo-oxidation of the polymeric materials (Feldman, 2002). Artificially weathering microplastics in the laboratory has been shown to aid researchers to achieve controlled aging of microplastics. Previously ultraviolet radiation (UV, 100–400 nm) has been applied to age microplastics (Almond et al., 2020; Fan et al., 2021; Liu et al., 2019; Mylläri et al., 2015; Wu et al., 2020). However, in the spectrum of solar irradiation, UV light accounts for only a small portion (~10 %) relative to the amount of visible light (Liu et al., 2021). Therefore, using visible light to age microplastics in the laboratory may be more environmentally relevant. The aging process of microplastics has been reported to enhance the adsorption of organic compounds on microplastics (Liu et al., 2020; Zhang et al., 2018). For this reason, conducting adsorption experiments using virgin microplastics may lead to an underestimation of the realistic adsorption potential of plastic particles in the environment. Furthermore, when in the environment, plastics can fragment into a range of sizes which can influence their interaction with micropollutants where they co-occur. Therefore, the investigation of various microplastic types and different size ranges should be more environmentally relevant when compared to studies conducted using a single plastic type and one size of particles. Along with microplastics, contaminants are often detected in freshwater systems as a mixture of compounds, including a variety of pharmaceuticals, the definition for which is prescription, over the counter, and veterinary therapeutic drugs used to prevent or treat human and animal diseases (Boxall et al., 2012). Pharmaceuticals have been detected in freshwater systems around the world (Fekadu et al., 2019). Due to the complexity of analysing pharmaceuticals in the environment and their potential impact on humans, wildlife, and ecosystems, these compounds have gained increased attention (Li et al., 2020). Carbamazepine was the pharmaceutical most frequently detected in river samples in a study that investigated 1052 sampling sites across 104 countries covering all continents (Wilkinson et al., 2022). Venlafaxine and fluoxetine were also included in the list of pharmaceuticals most commonly detected in rivers across the world. A review by Hughes et al. (2013) analysed the presence of 203 pharmaceuticals in freshwater ecosystems across 41 countries. According to the authors, the painkiller ibuprofen was consistently within the top five

identified compounds across all regions. Moreover, ibuprofen is often detected at higher concentrations, ranging from 0.02 to 3 $\mu\text{g L}^{-1}$ (Wang et al., 2019), among 16 pharmaceuticals evaluated in drinking waters from the UK. In Asia, the antibiotic ofloxacin was evident at concentrations up to 0.011 $\mu\text{g mL}^{-1}$ (Hughes, Kay and Brown, 2013). Furthermore, a range of pharmaceuticals including antibiotics (Li et al., 2018), and antidepressants (Wagstaff and Petrie, 2022) have been reported to adsorb onto microplastics.

The current study aimed to elucidate how a wide range of microplastic types, widely reported in the freshwater environment, interact with a mixture of pharmaceuticals when co-existing in the same aquatic environment. Two sizes, described as small ($D_{50} < 35 \mu\text{m}$) and large ($D_{50} 95\text{--}157 \mu\text{m}$), of six microplastics were, separately, placed in contact with a mixture of five pharmaceuticals with a range of hydrophobicities (Log K_{OW} 0.39–4.65). Additionally, virgin microplastics were artificially aged in the laboratory using simulated solar irradiation containing both UV and visible light to investigate the impact of the aging process of the microplastics on the adsorption of the selected pharmaceuticals.

2. Materials and methods

2.1. Materials and chemicals

Six microplastics types were commercially acquired from STGE (China). Microparticles of polypropylene (PP), polyethylene (PE), polyethylene terephthalate (PET), polyamide (PA), polystyrene (PS), and polyvinyl chloride (PVC) were purchased in two sizes, described in the current study as small and large particles (Fig. S1 and S2). Prior characterisation demonstrated a wide range of sizes for the material received (Moura et al., 2023). The particles received were sieved to standardise the size range of the particles using a shaker (AS200 Control Vibratory Sieve Shaker, RETSCH) at 1.5 mm amplitude for 10 min. The material described as small was retained between sieves of pore size 20 μm and 45 μm (ISO 3310/1, Fisher Scientific, UK), meanwhile the material described as large was retained between sieves of pore size 90 μm and 150 μm (ISO 3310/1, Fisher Scientific, UK). The small particles of PP and PVC were used as received as the majority of the particles were smaller than 20 μm (for particle size distribution see Fig. S3). The experimental medium consisted of artificial freshwater (AFW) with 0.02 % (w/v, 200 mg in 1 L) of sodium azide (NaN_3) used as a microbial inhibitor. The AFW and the 0.02 % NaN_3 were prepared with ultrapure water (18.2 M Ω). The AFW included $\text{CaCl}_2 \cdot 2\text{H}_2\text{O}$ (58.5 mg L^{-1}), $\text{MgSO}_4 \cdot 7\text{H}_2\text{O}$ (24.7 mg L^{-1}), NaHCO_3 (12.0 mg L^{-1}), and KCl (1.2 mg L^{-1}) according to (Akkanen and Kukkonen, 2003), and NaN_3 (200.0 mg L^{-1}). The pharmaceuticals ibuprofen (CAS RN 15687–27-1), carbamazepine (CAS 298–46-4), fluoxetine hydrochloride (CAS 56296–78-7), venlafaxine hydrochloride (CAS 99300–78-4), and ofloxacin (CAS 82419–36-1) were acquired from Tokyo Chemical Industry (UK) and were HPLC grade >97 % purity. Stock solutions at concentrations of 10 $\mu\text{g mL}^{-1}$ (10 mg in 1000 mL, carbamazepine), 20 $\mu\text{g mL}^{-1}$ (10 mg in 500 mL, ibuprofen), or 100 $\mu\text{g mL}^{-1}$ (10 mg in 100 mL, fluoxetine, venlafaxine, and ofloxacin) were prepared using AFW + 0.02 % NaN_3 depending on the pharmaceutical water solubility. No organic solvents were used to avoid cosolvent interference on the adsorption experiment. Prior to use, the stock solutions were stored at 4 °C in the dark. Due to the different molecular weights of the pharmaceuticals investigated in the current study, the initial concentration used was measured in moles per volume. The initial concentration of each pharmaceutical used was 16 $\mu\text{mol L}^{-1}$, which represents 5 $\mu\text{g mL}^{-1}$ of venlafaxine, chosen as a reference compound (Table 1). Although the initial concentration investigated (16 $\mu\text{mol L}^{-1}$) does not represent the pharmaceutical concentrations reported in the environment, high concentrations give insights regarding the interaction of pharmaceuticals with microplastics in the environment and enable the evaluation of the adsorption profile onto the microplastics.

2.2. Accelerated aging process of commercially acquired virgin microplastics

The commercially acquired virgin microplastics were aged using the SUNTEST XLS+ Xenon Arc weathering testing unit (ATLAS AMETEK Electronics Instrument Group, USA) equipped with a 1700 W Xenon Arc lamp operated at 60 W m^{-2} (300–400 nm) intensity, which irradiates a similar intensity of sunlight during summer ($\sim 1000 \text{ W m}^{-2}$ total irradiation, (Liu et al., 2021)). Microplastics (1 g) were placed into a beaker (200 mL) and exposed for 72 h. The samples were shaken every 24 h to ensure uniform exposure. The chamber temperature was maintained at $29.3 \pm 3.4 \text{ }^\circ\text{C}$ ($n = 2788$) using a cooling unit, however the high intensity of the irradiation caused the temperature of the samples to reach approximately $70 \text{ }^\circ\text{C}$ throughout the 72 h exposure. Increased temperatures lead to increased reaction rates and thermal degradation which accelerated the process of aging (Karlsson et al., 2018). Temperatures in some landfills and industrial composters have been reported to reach $80\text{--}100 \text{ }^\circ\text{C}$. Furthermore, it has been shown that accelerated degradation rates provided sufficient oxygen for the thermal-oxidative degradation (Chamas et al., 2020).

2.3. Characterisation of virgin and aged microplastics

The sieved virgin and aged microplastic particles were fully characterised, both to confirm the specifications provided by the manufacturer and to investigate how the aging process of the microplastics affected the particles. A Nicolet iS10 Fourier Transformer Infrared (FT-IR) Spectrometer (Thermo Fisher Scientific, UK) with OMNIC Spectra Software was used to investigate the chemical structure of the polymer. The FT-IR spectra were captured over the range 400 to 4000 cm^{-1} . Attenuated total reflectance (ATR) spectroscopy was used as the contact

sampling method. Thirty-two scans at a resolution of 8 cm^{-1} were collected to produce the spectra. No correction was applied. The carbonyl index (CI) was calculated from the area ratio of the integrated absorbance band of the carbonyl stretching ($\text{C}=\text{O}$) peak measured from 1850 to 1650 cm^{-1} and a reference peak (CH_2 , $1500\text{--}1420 \text{ cm}^{-1}$) that is not usually affected by the oxidation process (Almond et al., 2020) using eq. 1:

$$CI = \frac{\text{Area under band } 1,850 - 1,650 \text{ cm}^{-1} (\text{C}=\text{O})}{\text{Area under band } 1,500 - 1,420 \text{ cm}^{-1} (\text{CH}_2)} \quad (1)$$

The N_2 -BET adsorption-desorption surface area (S_{BET}) was determined using a Tristar II surface area and porosity instrument (Micromeritics, UK). Prior to the analysis, the microplastics were maintained under vacuum for 24 h using a VacPrep degasser (Micromeritics, UK) maintained at $30 \text{ }^\circ\text{C}$. This process removed surface adsorbed gas and moisture. Particle Size Analysis (PSA) was carried out using a Mastersizer 2000 particle size analyzer (Malvern Panalytical, UK). A simulated surface area (S_{PSA}) was calculated by the PSA software modelling the particles as perfect spheres and not accounting for the porosity and roughness of the material. Scanning Electron Microscopy (SEM, Scios DualBeam, Thermo Fisher Scientific, UK) was used to investigate the morphologies and to confirm the particle size of the microplastics. For crystallinity composition evaluation, powder X-Ray Diffraction (XRD) was carried out using an Empyrean diffractometer (Malvern Panalytical, UK) in reflection mode with a primary beam monochromator ($\text{Cu K}\alpha 1$). The calorimetric characteristics of the microplastics were measured using Differential Scanning Calorimetry (DSC) DSC250 (TA, USA) with N_2 as the purge gas. For this, microplastic (6.0 mg) was placed into an aluminium pan (TA, USA) and, sealed with an aluminium lid (TA, USA) using a Tzero Press (TA, USA). The pan, lid, and samples were handled using tweezers to avoid external interference with the sample weight. A

Table 1

Chemical structure, molecular weight, octanol-water partition coefficient ($\log K_{\text{OW}}$), pH dependant octanol – water partition coefficient ($\log D_{\text{OW}}$), acid dissociation constant (pK_a), and charge of ibuprofen, carbamazepine, venlafaxine hydrochloride, fluoxetine hydrochloride, and ofloxacin. Initial concentration (C_0) of each pharmaceutical that corresponds to $16 \mu\text{mol L}^{-1}$. Typically, $\text{pH} > pK_a$ (negatively charged); $\text{pH} \approx pK_a$ (neutral); $\text{pH} < pK_a$ (positively charged).

Pharmaceutical	Structure	Molecular weight (g mol^{-1})	C_0 ($\mu\text{g mL}^{-1}$)	$\log K_{\text{OW}} / \log D_{\text{OW}}^{**}$ (at pH 7)	pK_a^{***} (charge at pH 7)
Ibuprofen		206.29	3.29	3.97 / 4.85	4.85 ^a (-) ^b
Carbamazepine		236.27	3.76	2.45 / 2.45	- ^c (neutral) ^c
Venlafaxine hydrochloride		313.87	5.00	0.43 / -1.97	9.4 ^d (+)
Fluoxetine hydrochloride		345.78	5.51	4.05 / 1.25	9.80 ^a (+) ^e
Ofloxacin		361.37	5.76	-0.39 / -0.40	5.35 ^a ; 6.72 ^a (-) ^f

Values taken from: ^a (ChemAxon, 2023), ^b (Oh et al., 2016), ^c (Park et al., 2018), ^d (Sharma and Jain, 2009), ^e (Wagstaff et al., 2021), and ^f (Nurchi et al., 2019).

* Values taken from (NCCOS, 2021).

** Calculated as equation: $\log D_{\text{OW}} = \log K_{\text{OW}} - \log(1 + 10(pK_a - \text{pH}))$.

*** Note: Two pK_a values are shown when the pharmaceutical contains two different acidic functional groups, each of which can donate a proton to a solution.

sample without microplastic was prepared as a reference. To erase any thermal history effects, a heating-cooling-heating method was applied. For PP, PE, PET, PA, and PS, the first heating run was performed from 40 to 290 °C with a heating rate of 20 °C min⁻¹, followed by cooling from 290 to 0 °C at a cooling rate of 10 °C min⁻¹. The second heating run was from 0 to 290 °C at 10 °C min⁻¹. PVC showed degradation at 270 °C, therefore the first and second heating runs for PVC were limited to 250 °C. The degree of crystallinity (X_C) was calculated using eq. 2:

$$X_C = \frac{\Delta H_{m_{sample}} - \Delta H_{C_{sample}}}{\Delta H_{m_{100\%}}} \times 100 \quad (2)$$

where, $\Delta H_{m_{sample}}$ is the enthalpy change associated to the melting endotherm temperature (T_m) from the second heating run. $\Delta H_{C_{sample}}$ is the enthalpy change associated to the cold crystallisation exotherm temperature (T_c). $\Delta H_{m_{(100\%)}}$ is the reference value based on a 100 % crystalline polymer (Table S1).

Finally, the zeta potential of the virgin and aged plastics in experimental medium (AFW + 0.02 % NaN₃) was measured with a Malvern Zetasizer (Nano ZS, UK). The samples were measured between three and six times.

2.4. Adsorption experiment on virgin and aged microplastics

A solution containing a mixture of pharmaceuticals, each at 16 μmol L⁻¹, was placed in contact with one of the two sizes of the six microplastic types. All experiments and controls were conducted in triplicate. Samples were removed using a glass syringe with a stainless-steel needle (Hamilton, UK) to avoid contact of the pharmaceutical solution with laboratory plastics. The plastic particles (100 mg, equivalent to 2 g L⁻¹) were mixed with the pharmaceutical solutions (50 mL) in 100 mL Erlenmeyer flasks. Samples were continuously, horizontally agitated on a MaxQ 6000 orbital shaker (Thermo Scientific, UK) at 200 rpm for 48 h. Considering the particles as perfect spheres, for the plastic concentration investigated (2 g L⁻¹) this equates to approximately 10¹² (small PVC) to 10⁵ (large PA, see Table S2 parameters used for the estimated calculation) particles. The plastic concentration used in the current study does not represent the microplastic concentration reported in freshwater. However, it compares well with the plastic concentrations of published adsorption studies (Atugoda et al., 2021; Guo et al., 2019; Hüffer and Hofmann, 2016; Li et al., 2018; Petrie et al., 2023; Wagstaff et al., 2021; Wagstaff and Petrie, 2022; Xu et al., 2018), which enables a comparison to be made with data in the literature. The temperature was maintained at 25 °C in the dark. Samples (200 μL) were removed at 0.25, 1, 2, 4, 6, 10, 24, and 48 h using a 250 μL glass syringe with a stainless-steel needle (Hamilton, UK) and filtered using a microcentrifuge tube filter (2 mL spin-X tubes made of PP, cellulose acetate filter, 0.22 μm pore size, Corning USA). The samples were centrifuged for 30 s at 13,400 rpm (Mini-spin, Eppendorf, UK). The filtered samples (100 μL) were removed using a 100 μL glass syringe with a stainless-steel needle (Hamilton, UK), placed in 1.5 mL glass vials containing a microlitre glass insert (Kinesis, UK) then analysed by high performance liquid chromatography (HPLC) with photodiode array (PDA) detection. A control containing the mixture of pharmaceuticals without microplastic particles was also prepared and analysed at each sampling point. Throughout the investigation, contact with laboratory plastics was eliminated except for the microcentrifugation filtration device which could not be avoided. Controls indicated that the loss through this step was between 1 ± 0.5 % (venlafaxine) to 11 ± 4 % (fluoxetine). The adsorption was calculated on the basis of the difference in pharmaceutical concentration in the

samples with microplastics, and in the control (without microplastics, but including the pharmaceuticals).

2.5. Quantification of pharmaceuticals in solution using high performance liquid chromatography (HPLC)

Analysis of the pharmaceuticals was performed using high performance liquid chromatography (HPLC; Waters Corporation, UK). The equipment included a solvent delivery system (Alliance 2695) with photodiode array detection (PDA, Alliance 2996). The PDA scanning wavelength was set from 200 to 400 nm. Separation of the pharmaceuticals was achieved using a Symmetry dC18 column (2.1 mm internal diameter x 150 mm; 5 μm particles size) which was maintained at 40 °C. The mobile phases were ultra-pure water (18.2 MΩ) (A) and acetonitrile (B) each containing 0.05 % (v/v) trifluoroacetic acid (TFA; Fisher Scientific UK Ltd., UK). The flow rate was 0.3 mL min⁻¹. A linear gradient was used for the separation of the pharmaceuticals. Initial mobile phase composition of 90 % (A) was reduced to 20 % (A) over 21 min. A step gradient was used to reduce from 20 % (A) to 0 % (A). This was maintained for 5 min before returning to the starting conditions. Re-equilibration of the column was achieved by further elution of the column for 9 min prior to the next injection. The total run time was 35 min and the injection volume was 35 μL. The peak for Ibuprofen (220 nm), carbamazepine (285 nm), venlafaxine (226 nm), fluoxetine (227 nm), and ofloxacin (294 nm) was measured according to the maximum absorbance for each pharmaceutical within their respective UV absorption spectrum. The limit of detection and limit of quantification of the pharmaceuticals using this method was 0.01 μg mL⁻¹ and 0.05 μg mL⁻¹, respectively.

2.6. Data analysis

The amount of pharmaceutical adsorbed per unit mass of microplastic (μmol g⁻¹), was estimated using eq. 3:

$$q_{(t)} = \frac{(C_{ctrl(t)} - C_{(t)})V}{m} \quad (3)$$

where, $q_{(t)}$ is the amount of pharmaceutical adsorbed onto the microplastic (μmol g⁻¹) at sampling time t - $C_{ctrl(t)}$ is the control solution concentration of pharmaceutical (μmol L⁻¹) at the sampling time t as determined by HPLC-PDA- $C_{(t)}$ is the sample solution concentration of pharmaceutical (μmol L⁻¹) at the sampling time t as determined by HPLC-PDA- m is the mass of plastic added to the Erlenmeyer flask (g)- V is the total volume of solution (L) in the Erlenmeyer flask

The percentage of pharmaceutical adsorbed at a specific sample time point (t) onto the microplastic was calculated using eq. 4:

$$\%Adsorbed_{(t)} = \frac{(C_{ctrl(t)} - C_{(t)}) \times 100}{C_{ctrl(t)}} \quad (4)$$

where, $\%Adsorbed_{(t)}$ is the percent of pharmaceutical adsorbed on microplastics at sampling time t - $C_{ctrl(t)}$ is the control solution concentration of pharmaceutical (μmol L⁻¹) at the sampling time t as determined by HPLC-PDA- $C_{(t)}$ is the sample solution concentration of pharmaceutical (μmol L⁻¹) at the sampling time t as determined by HPLC-PDA

The total concentration of all pharmaceuticals adsorbed after the 48 h contact (μg mL⁻¹) was calculated using eq. 5:

$$\sum_{(48\ h)} = C_{Ibuprofen\ (48\ h)}^* + C_{Carbamazepine\ (48\ h)}^* + C_{Venlafaxine\ (48\ h)}^* + C_{Fluoxetine\ (48\ h)}^* + C_{Ofloxacin\ (48\ h)}^* \quad (5)$$

where, $\sum_{48\text{ h}}$ is the concentration of all pharmaceuticals in the mixture adsorbed after 48 h ($\mu\text{g mL}^{-1}$), $C_{\text{Pharmaceutical (48 h)}}$ is the amount adsorbed per unit mass of microplastic after 48 h ($\mu\text{g mL}^{-1}$) of each pharmaceutical in the mixture calculated using the difference in the pharmaceutical concentration in the control and the pharmaceutical concentration in the sample with microplastics. Note: * The concentration adsorbed onto microplastics that was not statistically different from the control ($p > 0.05$) was assigned a zero value.

Student's *t*-test was carried out to perform significance testing. For all statistical tests, a significance level of 5 % was set. A Pearson correlation matrix was performed to evaluate the correlation between variables of this study (Table S3). Correlation coefficient (r) > 0.7 was considered a strong positive association, while r lower than -0.7 was considered a strong negative association.

3. Results and discussion

3.1. Impact of the aging process on the microplastic properties

The nature of the microplastics can play an important role when it comes to the adsorption of organic compounds. The FT-IR analysis confirmed the polymer composition of the virgin microplastics that had been acquired commercially. In the current study, virgin microplastics were artificially aged by exposing the particles to the UV and visible light emitted by a Xenon Arc lamp. After 72 h irradiation, a colour change for both sizes of PS, PA, and PVC was observed. PS and PA showed a yellowing after the aging process, while PVC, especially the large particles, exhibited a change from white to a reddish-brown colour (Fig. S1 and S2). A change of colour of a plastic is a characteristic sign of polymer aging. PS yellowing has been attributed to the build-up of conjugated bond sequences in the polymer backbone (Yousif and Haddad, 2013). On the other hand, the reason for PA yellowing is thermal oxidation, during which pyrrole materials can be formed (He et al., 2014). Pyrrole, on exposure to air, is oxidised to highly coloured polymeric products (Ji Ram et al., 2019), resulting in the characteristic yellowing of PA. For PVC, the exposure of vinyl chloride polymers to light at 250–350 nm leads to the formation of characteristic discoloration from originally white to dark-brown or black (Yousif and Hasan, 2015). The photo- and thermal- degradation of PVC releases hydrogen chloride gas (dehydrochlorination), leading to the formation of conjugated polyene sequences ($-\text{CH}=\text{CH}-\text{CH}=\text{CH}-\text{CH}=\text{CH}-$) in the polymer chains, giving the PVC a reddish-brown colour (De Campos and Martins Franchetti, 2005; Hollande and Laurent, 1997). Extensive conjugation leads to colour. The longer the length of the conjugated segment, the greater the wavelength of the light that can be absorbed, eventually incorporating the wavelength range for visible light (380–700 nm, (Seidlitz et al., 2001).

The exposure of polymers to UV radiation causes photo-oxidative degradation which results in the breaking of the polymer chains which, in turn, can lead to the production of free radicals (Yousif and Haddad, 2013). FT-IR spectroscopy is one of the most common analytical techniques to monitor oxidative reactions (Almond et al., 2020). IR is particularly valuable for detecting polar functional groups, such as the carbonyl functional group for ketones and esters (intense peaks at 1715 cm^{-1} and 1735 cm^{-1} , respectively), which are typical of oxidative degradation pathways (Chamas et al., 2020) in plastics. A peak in the carbonyl function group IR absorption band ($1650\text{--}1800\text{ cm}^{-1}$) was detected in the samples of aged microplastics (Fig. 1). However, the FT-IR spectrum of small, virgin PP demonstrated a carbonyl functional group (C=O) peak at 1711 cm^{-1} (Fig. 1) that can be associated with either oxidised particles of PP or the presence of a grafting agent as discussed by Moura et al. (2023). The carbonyl peak formation cannot be observed for aged particles of PET due to the presence of an ester carbonyl intensive peak at 1712 cm^{-1} which is typical of PET. The amide peak (C-N + C=O) in the PA samples at 1635 cm^{-1} can also make the detection and measurement of a peak corresponding to carbonyl

functional groups in aged particles of PA difficult. Overall, the FT-IR spectra of the aged microplastics produced using the aging procedure in this study compare well with microplastic from environmental samples (Hendrickson et al., 2018; Veerasingam et al., 2021).

The carboxyl index (CI) is used to specifically monitor the absorption band of the carbonyl species formed during photo- or thermal-oxidation processes. The CI was calculated by measuring the ratio of the carbonyl peak ($1850\text{--}1650\text{ cm}^{-1}$), relative to a reference peak (Almond et al., 2020). For the current study, the C—H bending absorption was chosen as a reference peak ($1500\text{--}1420\text{ cm}^{-1}$) since it is typically not affected by the oxidation process. As expected, a greater CI was observed for aged microplastics when compared to virgin microplastics (Fig. 2), due to the formation of carbonyl functional groups caused by photo- and thermal-oxidation degradation. Overall, the large particles showed greater CI values when compared to the small particles. The size and the shape of the microplastics can affect the angle and how much radiation reaches each individual particle. These factors can affect the susceptibility of the particles to degradation. Individually, larger particles have a greater absolute surface area than smaller particles. Therefore, large microplastics have greater surface contact with the simulated solar radiation than small microplastics.

Most carbon-based polymers can degrade when exposed to sunlight in the presence of oxygen, however there is a wide range of photo-oxidative susceptibilities. In the current study, each microplastic type reacted differently to equivalent weathering conditions. The difference was more apparent on the large particles (Table 2). Large PVC demonstrated the greatest absolute increase in CI (2.48, Table 2) after artificial weathering (0.15 for virgin, large PVC, 2.63 for weathered, large PVC; Table 2) followed by PP (0.05 for virgin, large PP, 1.92 for weathered, large PP; Table 2). Much smaller increases in the CI were observed for large PS and PE on weathering. A small CI decrease was observed for both small and large PA on weathering (Fig. 2, Table 2). However, as previously mentioned, the amide peak in the PA samples at 1635 cm^{-1} can mask the detection and make it difficult the measurement of a peak corresponding to carbonyl functional groups in aged particles of PA.

Usually, the absorption of near-UV wavelengths (100–400 nm) leads to bond-breaking reactions and the concomitant loss of useful physical properties and/or discoloration (Yousif and Hasan, 2015). The initiation of polymer degradation by UV radiation depends mainly on the presence of UV-absorbing chromophores within the polymer (Tolinski, 2015). Microplastics with backbone chains constructed exclusively from carbon-carbon single bonds (C—C, e.g., PE) are less susceptible to photo-oxidative degradation due to the lack of UV-visible chromophores (Chamas et al., 2020). Although, PP also only contains carbon and hydrogen elements in its chemical structure, the different degradation encountered between PE and PP are due to presence of side methyl ($-\text{CH}_3$) groups in PP, which are absent in PE. The tertiary carbon atom present in PP particles is more prone to undergoing bond scission upon exposure to UV radiation, leading to the degradation of the polymer chains. As demonstrated by (Gijssman et al., 1999), the oxidation rate of PP was higher when compared to polybutylene terephthalate, followed by PA, while PE showed the lowest oxidation rate according to their oxygen uptake measured.

The majority of the microplastic types did not show a significant difference ($p > 0.05$) between the zeta potential of the virgin and the aged particles (Fig. 2 and Table 2). The microplastics that did show a significant difference were the small particles of PE, PA and PVC, and large PP. For all but small PVC, the zeta potential of the aged particles was more negative than the virgin particles (Fig. 2 and Table 2). The surface charge (zeta potential) of the microplastics varied from -10 mV (virgin, large PVC) to -64 mV (virgin, small PVC, Table 2). The small particles showed a greater surface charge when compared to the large particles (Fig. 2). (Nakatuka et al., 2015) demonstrated a clear correlation between the size of the particles and the zeta potential measurement. According to that study, particles of a small diameter are easily affected by the random movement of fluid flow and other particles. For

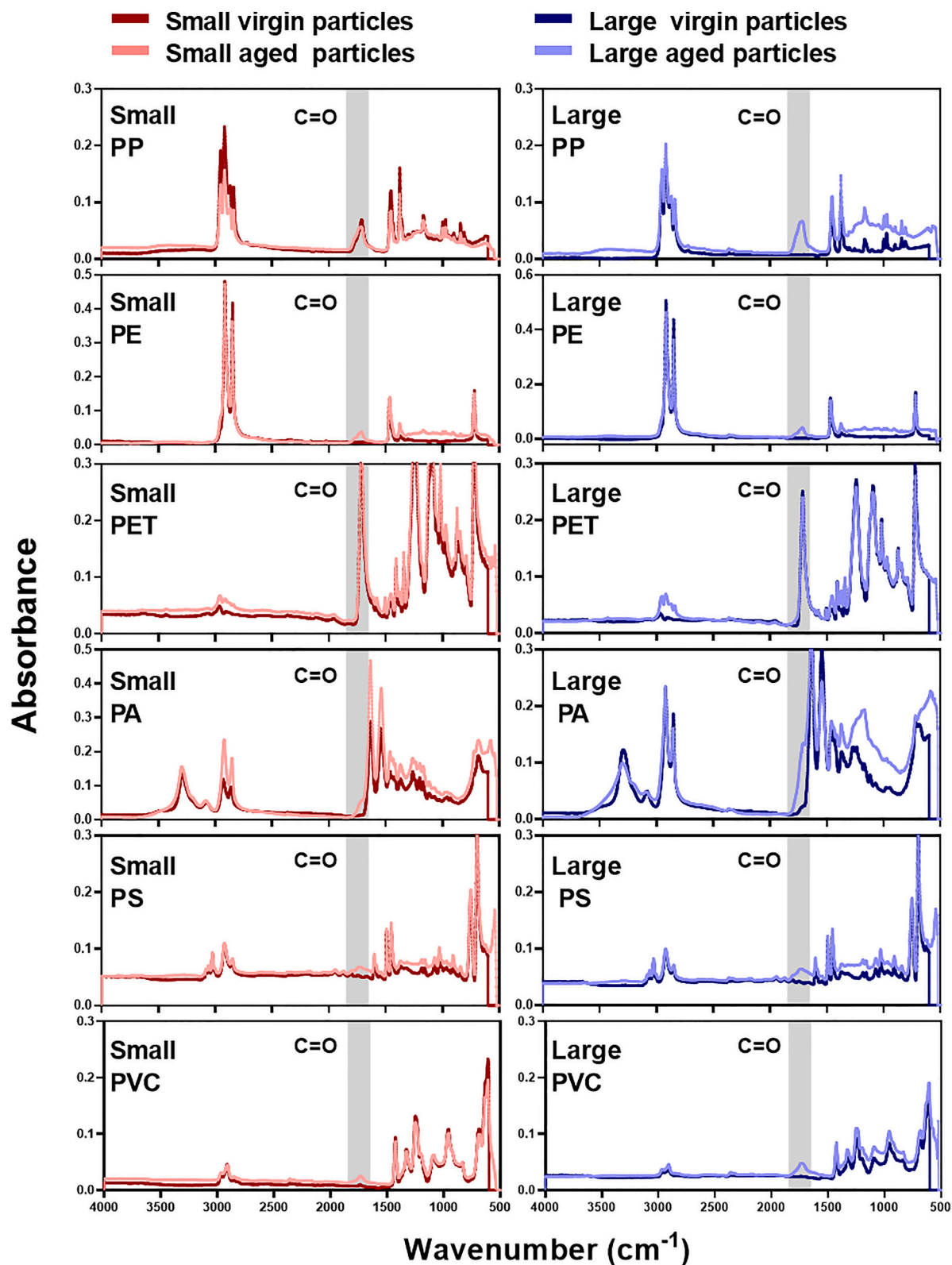


Fig. 1. Attenuated Total Reflectance Fourier Transformer Infrared (ATR FT-IR) spectra of virgin and aged polypropylene (PP), polyethylene (PE), polyethylene terephthalate (PET), polyamide (PA), polystyrene (PS), and polyvinyl chloride (PVC) described as small ($D_{50} < 35 \mu\text{m}$) and large ($D_{50} 95\text{--}157 \mu\text{m}$). Carbonyl functional group peak range ($1850\text{--}1650 \text{ cm}^{-1}$) highlighted in grey. A peak is evident in this highlighted region for the aged materials which contrasts with the virgin microplastics other than small PP (see text for further discussion on this aspect of the small, virgin PP spectrum). In some cases (e.g. PA) a peak shoulder is evident rather than a resolved peak. For PET the presence of a strong carbonyl peak in the virgin material masks any change that might have occurred in the spectrum of the aged material. Note the greater Y-axis values for PE and small PA.

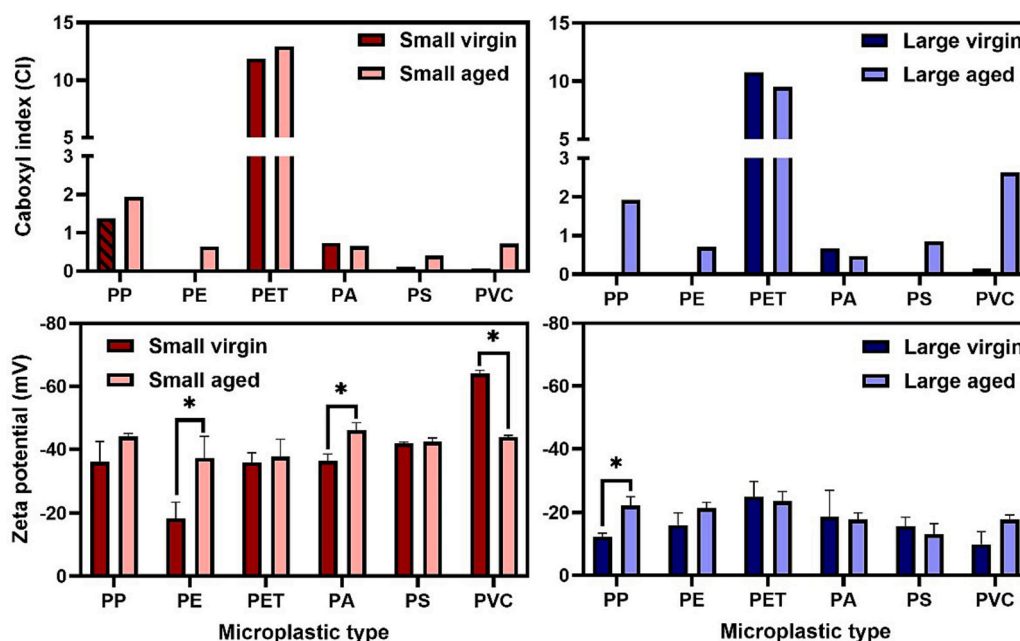


Fig. 2. Carboxyl index (CI) and zeta potential (ζ) measurement of virgin and aged polypropylene (PP), polyethylene (PE), polyethylene terephthalate (PET), polyamide (PA), polystyrene (PS), and polyvinyl chloride (PVC) described as small ($D_{50} < 35 \mu\text{m}$) and large ($D_{50} 95\text{--}157 \mu\text{m}$). The CI was calculated using eq. 1. *significant difference between the virgin and aged particles, $p < 0.05$. The large CI value for PET is because of the carbonyl ester grouping that is part of the polymer's composition. The hashed bar of small, virgin PP represents the untypical carbonyl functional group detected in its virgin particles. $n = 3$, errors bars = 1 standard deviation (SD).

this reason, the absolute value of effective zeta-potential of small particles is greater than that of large particles (Nakatuka et al., 2015).

The aging process of the microplastics did not appear to have caused the virgin particles to fragment. In fact, an aggregation of the particles was observed, especially for the small particles (PSA, Table 2; Fig. S3). Larger sized particles were recorded during the laser diffraction particle size analyses of the aged particles ($p < 0.05$, except large PE $p = 0.184$) when compared to the virgin particles (Table 2, see Table S4 for detailed statistical analysis). In addition, the aged microplastics were found to have a lower surface area (s_{BET}) when compared to the virgin microplastics (Table 2). Furthermore, no differences were visually apparent in the surface morphology of the microplastics due to the weathering when analysing the SEM images (Fig. S5 and S6). Moreover, no apparent difference in the glass transition temperature (T_g) was observed between the virgin particles and the aged particles (Table 2). The T_g is the temperature at which a plastic become soft (Alimi et al., 2018). Polymers with a T_g below the ambient temperature (25°C in this case) are considered rubbery polymers and include PP and PE (Table 2). In contrast, polymers with a T_g above ambient temperature (25°C in this case) are considered glassy polymers (e.g., PET, PA, PS, and PVC, Table 2). Apart from the large particles of PP, a discrete difference between the degree of crystallinity of the virgin microplastics when compared to the aged microplastics was observed. The material described as large PP demonstrated a decrease in the degree of crystallinity (X_c) from 47 % to 30 % (Table 2). Amorphous polymers such as PS and PVC do not contain crystalline regions. The melting point is the temperature at which the crystalline order is completely destroyed on heating (Chawla, 2012), therefore the absence of melting peaks in the DSC graphs of PS and PVC is expected (Fig. S7 and S8). The DSC analysis demonstrated that both sizes of PA consisted of different forms of PA. Small PA is a semi-crystalline polymer, while large PA is an amorphous form of PA. That highlights the need for a detail characterisation of commercial microplastics to ensure reliable data interpretation as discussed by Moura et al., 2023.

3.2. Differential adsorption of the five pharmaceuticals by the six microplastics

The interaction of pharmaceuticals with microplastics is multifactorial in nature. In the current study, the properties of the pharmaceutical, the type of microplastic, and the microplastic weathering were all key factors affecting this interaction. Results demonstrated that fluoxetine was the pharmaceutical that was most readily adsorbed by the microplastics (Fig. 3), with aging generally increasing the adsorption by the microplastics. Among the microplastic types investigated, PET showed minimal adsorption, even after aging of the particles (Fig. 3). In the mixture of the five pharmaceuticals, fluoxetine was the only compound to be adsorbed by virgin particles of small PA ($56 \pm 4\%$ adsorption after 48 h) and large PA ($45 \pm 4\%$ adsorption after 48 h). Furthermore, fluoxetine was adsorbed in greater amounts on small, virgin PVC ($71 \pm 3\%$ adsorption) and small virgin PE ($8 \pm 2\%$ adsorption) relative to some of the other pharmaceuticals such as venlafaxine ($8 \pm 1\%$ adsorption on small, virgin PVC) and ibuprofen ($4 \pm 1\%$ adsorption on small, virgin PE). Although ofloxacin appeared to adsorb $8 \pm 8\%$ on small, virgin PVC, no significance difference was observed when compared to the control after 48 h contact ($p = 0.24$). Furthermore, while all pharmaceuticals investigated adsorbed on virgin particles of small PP, fluoxetine showed the greatest adsorption (97 %), while ibuprofen and carbamazepine demonstrated the lowest adsorption (16 %). Interestingly, there was a difference in the adsorption of venlafaxine by virgin and aged small PP. After 48 h, the adsorption of fluoxetine and venlafaxine was similar for the virgin particles (approximately $4 \mu\text{g mL}^{-1}$ adsorption each), but different for the aged particles. Fluoxetine adsorbed similar amounts onto aged PP ($4.06 \pm 0.06 \mu\text{g mL}^{-1}$), while venlafaxine adsorbed in lower amounts ($2.00 \pm 0.09 \mu\text{g mL}^{-1}$) compared to the small, virgin PP particles (Table 3).

Studies have shown that the hydrophobicity of organic compounds plays an important role regarding the adsorption on microplastics (Prajapati et al., 2022). The partition coefficient between octanol and water ($\log K_{OW}$) is a physicochemical parameter widely used to describe the hydrophobic properties of a compound (De Bruijn et al., 1989). The

Table 2

Mean particle size analysis (PSA, $n = 3$) range, mean median particle size (D_{50}), mean simulated surface area (s_{PSA}), N_2 adsorption-desorption surface area (s_{BET} , $n = 1$), glass transition temperature (T_g) measured by differential scanning calorimetry (DSC, $n = 1$), degree of crystallinity (X_c) calculated using eq. 2, mean zeta potential (ζ , $n = 3$), and carboxyl index (CI, $n = 1$) calculated using eq. 1 for virgin and aged particles, described as small and large, of polypropylene (PP), polyethylene (PE), polyethylene terephthalate (PET), polyamide (PA), polystyrene (PS) and polyvinyl chloride (PVC). *Note: There are two PSA ranges for PVC due to the fact that on analysis there were found to be two distinct size distributions (Fig. S3). - not applicable for amorphous polymers.

	PSA range	D_{50}	s_{PSA}	s_{BET}	T_g	X_c	ζ	CI
	μm	μm	$\text{area m}^2 \text{g}^{-1}$	$\text{area m}^2 \text{g}^{-1}$	$^{\circ}\text{C}$	%	mV	-
Virgin plastic –								
Small particles								
PP	4–23	8	0.72	52.2	<0	32	–36	1.38
PE	3–209	24	0.31	1.5	<0	15	–18	0.02
PET	10–91	29	0.22	0.8	81	23	–36	11.87
PA	1–105	33	0.27	0.6	91	9	–36	0.74
PS	2–91	26	0.30	1.6	95	–	–42	0.12
PVC (1)	0.04–0.3							
PVC (2)	0.5–4	0.14	43.50	4.3	84	–	–64	0.06
Aged plastic –								
Small particles								
PP	52–976	22	0.31	49.29	<0	30	–44	1.94
PE	4–976	127	0.09	1.10	<0	20	–37	0.64
PET	10–59	30	0.21	0.38	89	22	–38	12.94
PA	3–976	107	0.08	0.23	91	10	–46	0.65
PS	2–976	42	0.17	0.69	94	–	–42	0.41
PVC (1)								
PVC (2)	1–163	7	1.11	2.89	84	–	–44	0.72
Virgin plastic –								
Large particles								
PP	60–216	134	0.05	0.01	<0	47	–12	0.05
PE	60–478	157	0.04	0.28	<0	17	–16	0.02
PET	3–216	95	0.09	0.28	81	19	–25	10.78
PA	46–240	105	0.06	0.92	22/94	–	–19	0.68
PS	60–263	134	0.05	0.39	96	–	–16	0.06
PVC	52–240	107	0.053	0.41	83	–	–10	0.15
Aged plastic –								
Large particles								
PP	46–240	127	0.05	0.03	<0	29	–22	1.92
PE	52–254	158	0.04	0.07	<0	22	–21	0.71
PET	10–272	103	0.07	0.10	81	23	–24	6.52
PA	40–976	252	0.03	0.08	89	–	–18	0.48
PS	46–186	108	0.06	0.23	97	–	–13	0.85
PVC	52–976	119	0.05	0.07	83	–	–18	2.63

greater the $\log K_{OW}$ value, the greater the hydrophobicity of the compound (Thermo Scientific, 2007). For the five pharmaceuticals studied, fluoxetine has the greatest $\log K_{OW}$ (4.05), while ofloxacin has the lowest (–0.39, Table 1) based on literature data (NCOSS, 2021). However, the pH of the test or environmental system is important because as the pH changes, the state of ionisation changes and this will have an impact on adsorption. Most pharmaceuticals are ionisable, with the extent of their ionisation varying with the pH of the media (Wagstaff et al., 2021). This needs to be taken into account when considering the environmental fate of such compounds and is done using the pH dependent octanol-water partition coefficient ($\log D_{OW}$). The pH of the experimental media was pH 7. The consequence of this for the hydrophobicity of fluoxetine is that it decreases markedly ($\log D_{OW}$ 1.25). At pH 7, ibuprofen is the most hydrophobic ($\log D_{OW}$ 4.85) and venlafaxine is least hydrophobic compound in the mixture ($\log D_{OW}$ – 1.97, Table 1).

Although the virgin particles of small PE ($r = 0.83$) showed a strong positive correlation with $\log K_{OW}$ (Table S3, Fig. 4), small amounts of fluoxetine ($0.31 \pm 0.06 \mu\text{g mL}^{-1}$) and ibuprofen ($0.12 \pm 0.03 \mu\text{g mL}^{-1}$) adsorbed onto small, virgin PE (Table 3, Fig. S9). A strong correlation of virgin small PS with pH dependent coefficient ($\log D_{OW}$ 0.77) for the five pharmaceuticals was also observed. Virgin small PP, on the other hand, presented a strong, negative correlation ($r = -0.81$) when compared with the $\log D_{OW}$ of the pharmaceuticals investigated. Apart from those, no correlation was observed when comparing the adsorption of each pharmaceutical with their respective $\log K_{OW}$ and $\log D_{OW}$ (Table S3). This means that the hydrophobicity of the pharmaceuticals may not be the major driving factor regarding their interaction with microplastics, and other adsorption mechanisms, such as electrostatic interactions,

may be more important.

Electrostatic and hydrophobic attractions play a significant role in the marked uptake of fluoxetine on microplastics (Atugoda et al., 2021). At pH 7, fluoxetine and venlafaxine are positively charged, ibuprofen and ofloxacin are negatively charged, and carbamazepine is uncharged (Table 1). The positive charge of fluoxetine at pH 7 and the negatively charged surface of microplastics makes electrostatic interaction favourable (Table 2, Fig. 2). Although, venlafaxine is also positively charged at the experimental media pH, its hydrophilicity can have a negative impact on the adsorption onto microplastics, especially when co-occurring with highly hydrophobic and also cationic compounds such as fluoxetine. (Moura et al., 2022) has demonstrated that hydrophobic compounds can compete for binding sites and be adsorbed in greater amounts when placed in a mixture with more hydrophilic compounds. Fluoxetine has been reported to be adsorbed in greater amounts on PA microparticles when compared to the cationic (positively charged) pharmaceuticals atenolol, pseudoephedrine, metoprolol, tramadol, propranolol, and amitriptyline (Wagstaff et al., 2021).

3.3. The effect of the physico-chemical characteristics of microplastics on the adsorption of pharmaceuticals

The type of microplastics can affect the adsorption behaviour of pharmaceuticals by microparticles. In the current study, the total amount of the pharmaceuticals adsorbed by the microplastics varied according to the polymer (Fig. 5). Additionally, the adsorption behaviour for each pharmaceutical depended on the type of microplastic. Small PP showed the greatest adsorption among the microplastics

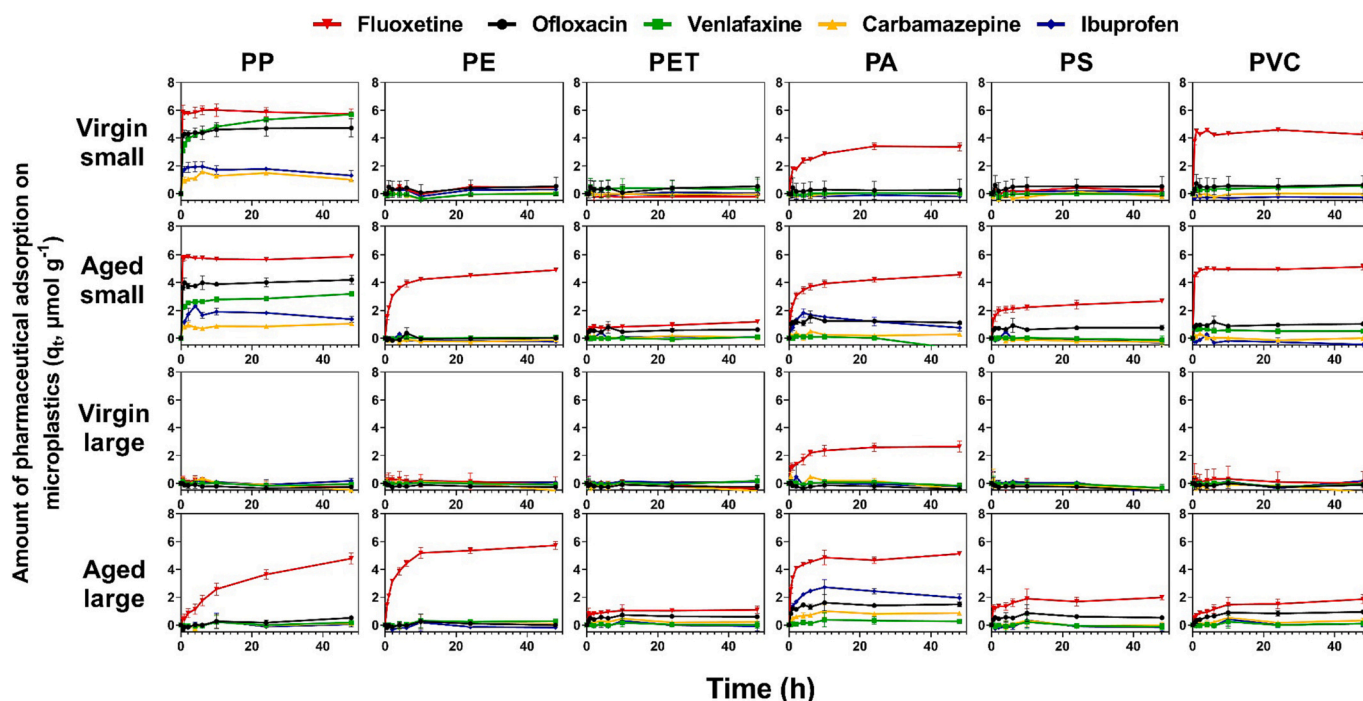


Fig. 3. Amount of pharmaceutical adsorbed onto small ($D_{50} < 35 \mu\text{m}$) and large ($D_{50} 95\text{--}157 \mu\text{m}$) polypropylene (PP), polyethylene (PE), polyethylene terephthalate (PET), polyamide (PA), polystyrene (PS), and polyvinyl chloride (PVC) over 48 h in a mixture of five pharmaceuticals on the basis of size (small or large) and the nature of the microplastics (virgin or aged). $n = 3$, errors bars = 1 SD. The amount adsorbed (q_t) was calculated using eq. 3. The control consisted of a mixture of the five pharmaceuticals without microplastics. In short, fluoxetine readily adsorbed on microplastics; aging has a marked impact on the adsorption; PET shows very little adsorption even after aging.

investigated, followed by PA. In the mixture, the virgin particles of small PP adsorbed from 16 % (ibuprofen and carbamazepine) to 97 % (fluoxetine). A similar adsorption capacity is observed by the aged particles of small PP. For the small virgin particles, only PP, PA, and PVC showed a marked adsorption of fluoxetine with varying amounts of the other pharmaceuticals being adsorbed (Fig. 3). Meanwhile, no significant adsorption ($p > 0.05$) was observed comparing the concentration of all pharmaceuticals in the mixture in contact with small, virgin PET to their concentrations in the control after 48 h contact. For small, virgin PS, a small amount of ibuprofen (2 ± 1 % adsorption) demonstrated a significant difference ($p = 0.02$) from the control after 48 h contact. A discrete adsorption was also observed by small, virgin PE, where fluoxetine and ibuprofen adsorbed 8 ± 2 % ($p = 0.02$) and 4 ± 1 % ($p = 0.02$) onto small PE, respectively. There is a marked increase in adsorption of the pharmaceuticals by the small particles following aging. When considering the combined amount (\sum_{PHA}) of all pharmaceuticals in the mixture, except for PP, the small particles demonstrated a significantly greater ($p < 0.05$) adsorption on aged particles when compared to the amount of pharmaceuticals adsorbed on the virgin microplastics (Fig. 5).

Considering the virgin microplastics, the size of the particles affected the amount adsorbed on the microplastics. Overall, the small, virgin microplastics showed greater adsorption of the pharmaceuticals when compared to the large, virgin particles. Minimal adsorption of pharmaceuticals was observed by the large virgin particles, except for large PA that stands out for its adsorption of fluoxetine (45 % adsorption). Large PA is an amorphous form of PA, like PS and PVC that are typically amorphous. Amorphous polymers, in which crystalline regions are absent, are expected to show greater adsorption when compared to more crystalline polymers (Seo et al., 2022). Furthermore, large PA has the greatest s_{BET} ($0.92 \text{ m}^2 \text{ g}^{-1}$) when compared to the other large microplastics ($0.01\text{--}0.41 \text{ m}^2 \text{ g}^{-1}$, Table 2). The combination of the polar nature, greater surface area, and amorphous properties of large PA might explain why fluoxetine, a hydrophobic compound, showed a marked

adsorption onto the large PA particles.

For PP and PVC, the size of the particles is not the only factor affecting the adsorption when compared to the larger particles of the same microplastic type. For small PP, the presence of the carbonyl functional group (C=O) in the IR spectrum that is not present in the large particles of PP (Fig. 2) and its comparatively large surface area ($s_{\text{BET}} 52.2 \text{ m}^2 \text{ g}^{-1}$) affects the adsorption of small PP. Although, unmodified PP is typically a non-polar polymer, the presence of the carbonyl functional group (C=O) in the virgin particles of small PP will likely have an impact. Polar polymers usually contain polar functional groups, such as hydroxyl (-OH), carboxyl (-COOH), or amino (-NH₂) groups, which create regions of partial positive and negative charges within the polymer structure. These charged or polar regions can interact with hydrophilic compounds through intermolecular forces such as hydrogen bonding, $\pi\text{-}\pi$ interactions, or ion- π interactions. As a result, organic compounds can more easily adsorb onto the surface of polar polymers due to these attractive forces. Furthermore, the greater surface area, the greater adsorption expected (Chen et al., 2013). The large surface area of small PP suggests that along with electrostatic and hydrophobic interactions, pore filling was the main mechanism of adsorption taking place in the interaction of small PP with the pharmaceuticals, as also demonstrated by (Moura et al., 2022). Likewise, for small PVC, the small particle size (Table 2) and the spongy surface morphology of the particles might have additional effects on the interaction with the pharmaceuticals when compared to the smooth surface morphology of large PVC (Fig. S6). Moreover, the polar surface and increased s_{BET} of small PP and PVC ($s_{\text{BET}} 4.3 \text{ m}^2 \text{ g}^{-1}$) affect the dispersion of the particles through the water column, which might be the reason that the adsorption of pharmaceuticals onto these virgin and aged microplastics rapidly attains a plateau when compared to non-polar and less porous microplastics, such as large PP and PE (Fig. 3). The s_{BET} showed a stronger positive correlation when compared to the total amount adsorbed onto virgin ($r = 0.97$) and aged ($r = 0.83$) microplastics (Table S3). That means that other interaction mechanisms such

Table 3

Concentration of each pharmaceutical adsorbed onto small ($D_{50} < 35 \mu\text{m}$) and large ($D_{50} 95\text{--}157 \mu\text{m}$) polypropylene (PP), polyethylene (PE), polyethylene terephthalate (PET), polyamide (PA), polystyrene (PS), and polyvinyl chloride (PVC) after 48 h contact in a mixture of five pharmaceuticals on the basis of size (small or large) and the nature of the microplastics (virgin or aged). $n = 3$, mean \pm SD. The concentration adsorbed was calculated using the difference between the pharmaceutical concentration in the control and the pharmaceutical concentration in the sample with microplastics.

Concentration adsorbed onto microplastics ($\mu\text{g mL}^{-1}$)					
Small plastic					
Virgin plastics					
PP	3.42 \pm 0.39	3.57 \pm 0.08	0.47 \pm 0.06	3.96 \pm 0.2	0.54 \pm 0.13
PE	–	–	–	0.31 \pm 0.06	0.12 \pm 0.03
PET	–	–	–	0.02 \pm 0.01	–
PA	–	–	–	2.33 \pm 0.17	–
PS	–	–	–	–	0.07 \pm 0.01
PVC	–	0.35 \pm 0.06	–	2.94 \pm 0.16	–
Aged plastics					
PP	3.03 \pm 0.19	2 \pm 0.09	0.5 \pm 0.06	4.06 \pm 0.06	0.56 \pm 0.08
PE	–	–	–	3.39 \pm 0.05	–
PET	0.45 \pm 0.03	–	–	0.82 \pm 0.08	0.03 \pm 0.01
PA	0.8 \pm 0.09	–	0.13 \pm 0.01	3.16 \pm 0.12	0.31 \pm 0.08
PS	0.54 \pm 0.1	–	–	1.85 \pm 0.02	–
PVC	0.74 \pm 0.08	0.32 \pm 0.05	–	3.55 \pm 0.12	–
Large plastic					
Virgin plastics					
PP	–	–	–	–	–
PE	–	–	–	–	–
PET	–	–	–	–	–
PA	–	–	–	1.83 \pm 0.28	–
PS	–	–	–	–	–
PVC	–	–	–	–	–
Aged plastics					
PP	0.37 \pm 0.03	–	–	3.31 \pm 0.22	–
PE	–	–	–	3.96 \pm 0.16	–
PET	0.43 \pm 0.09	–	–	0.75 \pm 0.15	–
PA	1.07 \pm 0.11	0.16 \pm 0.05	0.4 \pm 0.06	3.54 \pm 0.06	0.81 \pm 0.1
PS	0.38 \pm 0.06	–	–	1.37 \pm 0.09	–
PVC	0.68 \pm 0.08	–	–	1.28 \pm 0.18	–

- no adsorption evident.

Note: When the amount adsorbed onto the microplastics was not statistically different from the control ($p > 0.05$) a zero value was assigned.

as electrostatic interactions are in place along with s_{BET} when pharmaceuticals are placed in contact with aged microplastics.

In addition to the density of the microplastics, the hydrophobicity of microplastics also plays an important role regarding the buoyancy of the particles in the water column. Less dense and hydrophobic microplastics such as PS, PE, and PS (Table S1) tend to float when in contact with water, which can decrease the surface area in contact with organic compounds dissolved in the liquid phase. The decreased surface contact can lower the adsorption potential of the hydrophobic microplastic. Polarity might be the main reason that the microplastics which are considered polar polymers investigated in the current study (e.g., small PP, PA, and PVC) showed the greatest adsorption of the pharmaceuticals onto the virgin particles when compared to non-polar polymers (PP, PE, and PS).

3.4. The effect of aging on the adsorption of pharmaceuticals by microplastics

The weathering of microplastics had clear consequences for the adsorption of pharmaceuticals by microplastics. In the current study, artificially aged microplastics showed greater adsorption when compared to the virgin particles for both microplastic sizes (Fig. 3 and Fig. 5). The large particles of all microplastic types showed significantly greater adsorption ($p < 0.05$) by the aged particles compared to the virgin particles. For example, the large particles of PA demonstrated a

marked increase in the adsorption of pharmaceuticals between the virgin ($\sum_{\text{PHA}} 1.83 \pm 0.28 \mu\text{g mL}^{-1}$) and aged ($\sum_{\text{PHA}} 5.99 \pm 0.25 \mu\text{g mL}^{-1}$) material (Table 3). In this case the increased adsorption was due to changes in the adsorption of all five pharmaceuticals ($p < 0.05$). This contrasts with PE which, although it showed a significant increase in adsorption, the change was almost entirely due to an increase in the adsorption of fluoxetine (Fig. 3).

As highlighted, fluoxetine consistently was the pharmaceutical that was most readily adsorbed by the microplastics, the adsorption being enhanced by aging. Only fluoxetine adsorbed ($78 \pm 3 \%$) on large, aged PP, while virgin particles of large PP did not adsorb any of the pharmaceuticals in the mixture (Fig. 3). However, fluoxetine was not the only pharmaceutical to be adsorbed onto the aged particles. Ibuprofen, and ofloxacin were adsorbed by aged particles of both sizes of PA (Fig. 3). Aging also enhanced the adsorption of ofloxacin by PS and PET relative to the virgin particles, ofloxacin showed the second highest absolute adsorption after fluoxetine. However, lower amounts of fluoxetine and ofloxacin adsorbed on aged PET when compared to aged PS. In general, aging increases the adsorption of less hydrophobic/hydrophilic organic compounds on microplastics (Prajapati et al., 2022). (Liu et al., 2019) have also reported an increase in the adsorption of the hydrophilic antibiotic ciprofloxacin ($\log K_{OW} 0.4$) onto PS and PVC microparticles (size $\sim 70 \mu\text{m}$). The authors suggested the adsorption on microplastics is not limited to hydrophobic organic compounds, especially due to the increasing number of oxygen-containing functional groups present in aged particles ((Liu et al., 2019). Carbonyl functional groups contain a carbon which has a partial positive charge, while the oxygen has a partial negative charge. The positive charge of the carbonyl carbon might favour the electrostatic interaction of anionic (negatively charged) pharmaceuticals such as ibuprofen and ofloxacin (Table 1).

Aging clearly changes the adsorption potential for the large particles, especially in respect of fluoxetine. The results indicate that the size of the microplastics can be a secondary factor affecting the adsorption when compared to the weathering of the particles. Considering the combined amount (\sum_{PHA}) of the all pharmaceuticals adsorbed, the aged particles of small PA ($\sum_{\text{PHA}} 3.85 \pm 0.85 \mu\text{g mL}^{-1}$) adsorbed in significant lower amounts ($p = 0.01$) when comparing with large, aged PA ($\sum_{\text{PHA}} 5.99 \pm 0.25 \mu\text{g mL}^{-1}$). Likewise, large, aged PE ($\sum_{\text{PHA}} 3.96 \pm 0.19 \mu\text{g mL}^{-1}$) showed significant greater adsorption ($p = 0.02$) of pharmaceuticals in comparison to aged particles of small PE ($\sum_{\text{PHA}} 3.39 \pm 0.06 \mu\text{g mL}^{-1}$, Fig. 5, Table 3). Along with the size of the particles, properties such as glassiness, crystallinity and the polarity of microplastics have shown to impact the adsorption behaviour of organic compounds. (Liu et al., 2019). In the current study, the polarity of both virgin and aged microplastics had a considerable impact on the adsorption of the pharmaceuticals. For instance, small PP (that contains a carbonyl functional group), PA, and PVC, considered polar polymers, were the virgin microplastic types that showed greatest adsorption of the pharmaceuticals investigated (Fig. 3 and Fig. 5). Furthermore, due to photo-oxidation and weathering, microplastics, including the non-polar polymers (e.g., PP, PE, and PS), develop polar oxygen-containing groups that can favour hydrogen bond interaction (Prajapati et al., 2022) along electrostatic and hydrophobic interactions. The absence of oxygen-containing groups that favour those interactions might be the reason that, for both sizes of virgin PE, there was no adsorption of the pharmaceuticals, while fluoxetine was adsorbed on small (82 %) and large (93 %) particles of aged PE. According to (Li et al., 2018), the formation of hydrogen bonding was the key mechanism underlying the high adsorption of the hydrophilic antibiotics amoxicillin, tetracycline, and ciprofloxacin on PA. However, H-bonding interactions are weaker compared to hydrophobic and electrostatic interactions (Prajapati et al., 2022). Aliphatic polymers, such as PE and PVC, normally undergo van der Waals interactions, while aromatic polymers, such as PS, is usually attributed to π - π interactions (Tourinho et al., 2019).

Several studies have also observed an increase in the adsorption of organic compounds on aged microplastics when compared to virgin

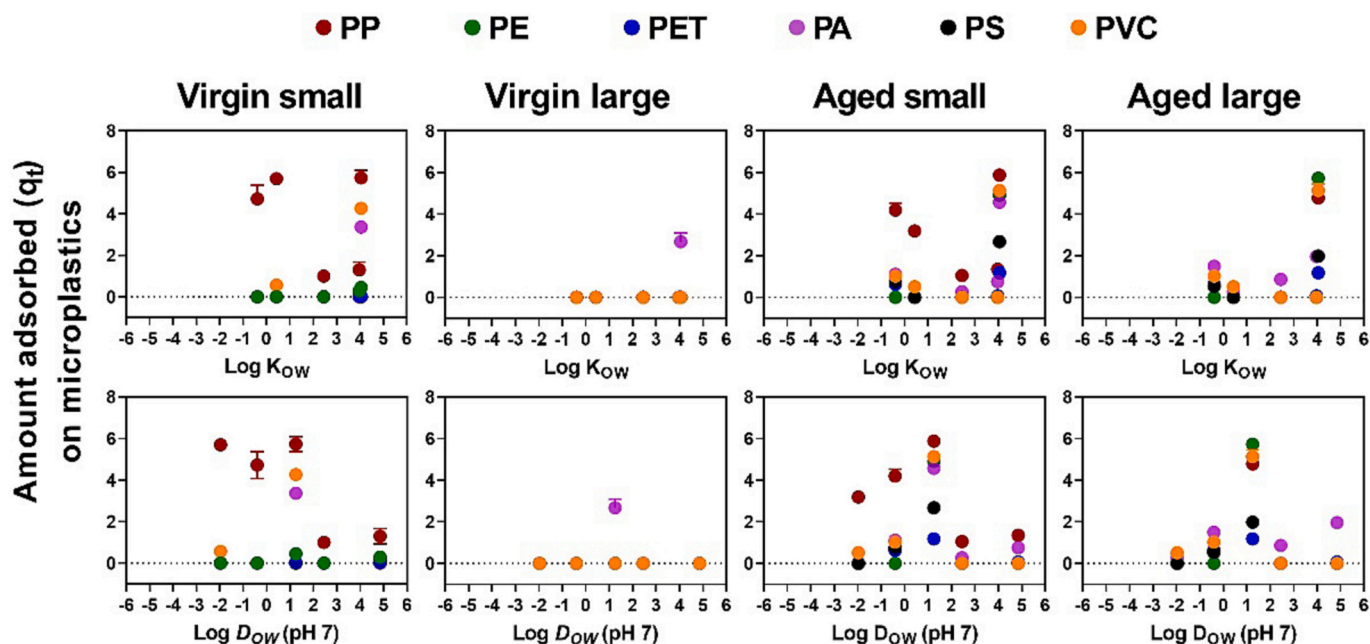


Fig. 4. Comparison of the amount of pharmaceutical adsorbed onto microplastics after 48 h with the octanol-water partition coefficient ($\log K_{OW}$, Table 1) and the pH dependent octanol-water partition coefficient ($\log D_{OW}$ at pH 7, Table 1). The material described as small ($D_{50} < 35 \mu\text{m}$) and large ($D_{50} 95\text{--}157 \mu\text{m}$) of polypropylene (PP), polyethylene (PE), polyethylene terephthalate (PET), polyamide (PA), polystyrene (PS), and polyvinyl chloride (PVC) after 48 h in a mixture of five pharmaceuticals was compared on the basis of size (small or large) and the weathering of the microplastics (virgin or aged). $n = 3$, errors bars = 1 SD. The amount adsorbed (q_t) was calculated using eq. 3. A zero value was attributed to the q_t when the adsorption was not significantly different ($p > 0.05$) from the control.

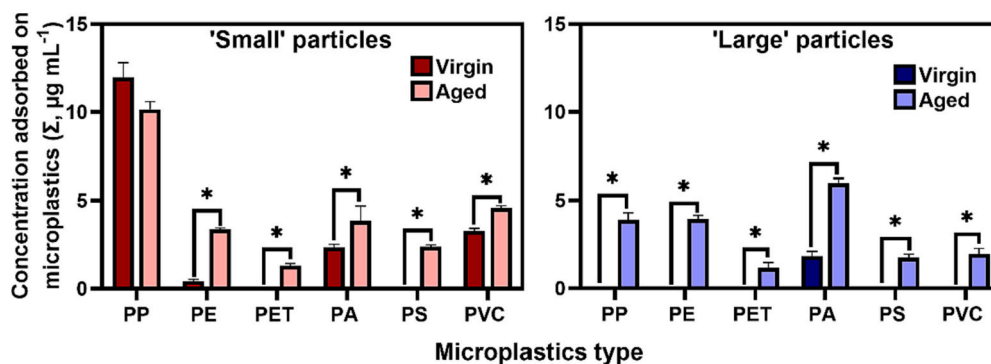


Fig. 5. Total concentration of pharmaceuticals (Σ_{PHA}) adsorbed onto small ($D_{50} < 35 \mu\text{m}$) and large ($D_{50} 95\text{--}157 \mu\text{m}$) polypropylene (PP), polyethylene (PE), polyethylene terephthalate (PET), polyamide (PA), polystyrene (PS), and polyvinyl chloride (PVC) after 48 h in contact with a mixture of the pharmaceuticals on the basis of size and the nature of the microplastics (virgin and aged). $n = 3$, errors bars = 1 SD. The total concentration adsorbed (Σ_{PHA}) was estimated using eq. 5. The control consisted of a mixture of the five pharmaceuticals without microplastics. *significant difference between the virgin and aged particles, $p < 0.05$.

microplastics (Bhagat et al., 2022; Hüffer et al., 2018; Liu et al., 2020; Zhang et al., 2018). The increase in the adsorption capacity of the aged particles can be explained by the change in the hydrophobicity and the surface charge caused by thermal- and photo-oxidation processes. According to (Atugoda et al., 2021), the aging of microplastics decreases the hydrophobicity and increases the electrostatic interactions between the aged microplastics and pharmaceutical compounds, resulting in their retention on the polymer. The addition of polar, oxygen-containing functional groups to the surface results in a trend towards higher hydrophilicity and surface free energy of microplastics (Bhagat et al., 2022).

4. Environmental implications of this study

Most studies on the adsorption of aquatic pollutants onto microplastics have used virgin microplastics. However, microplastics acquired commercially might not be representative of what is detected in the

environment. This is especially the case when using perfectly spherically-shaped microplastics which only represent 14 % of the microplastic type reported in the freshwater environment (Koelmans et al., 2019). In the current study, a wide range of microplastic types with different sizes and shapes were evaluated to achieve a better representation of the microplastic found in the aquatic environment. However, simulating the physico-chemical and biological processes particles undergo when in the environment is a challenge. Artificially aging microplastics is a multifactorial process. The degree of weathering of polymers depends on type and the intensity of light source, the presence/absence of water and the ambient temperature. Particles have been aged in the laboratory using a variety of light sources, radiation intensities, and exposure times. The most commonly used types of light sources to age microplastics, to date, are UV-based (UV-A, -B, and -C, 100–400 nm, (Almond et al., 2020; Fan et al., 2021; Liu et al., 2019; Mylläri et al., 2015; J. Wu et al., 2020)). However, UV light only accounts for the small portion (~10 %) of sunlight when compared to the amount

of visible light (Liu et al., 2021). For these reasons, a combination of UV and visible light sources such as Xenon Arc lamps might be a better representation of microplastics exposure to sunlight. Furthermore, a detailed characterisation is crucial to achieve full understanding of the virgin microplastics received by the suppliers and to understand how aging impacts the chemical structure, surface morphology, particle size, surface charge and crystallinity of microplastics as discussed previously (Moura et al., 2022).

The pharmaceuticals investigated in this study have high prescription rates globally and low biodegradability in the environment. They are also widely reported in the freshwater environment (Fekadu et al., 2019). Micropollutants such as pharmaceuticals are often detected as a mixture in freshwater systems (Ebele et al., 2017). The majority of adsorption studies to date evaluate individual compounds in contact with microplastics. Although it is important to understand how organic micropollutants interact individually with microplastics, this approach does not consider potential intramolecular adsorption competition (Moura et al., 2022). As confirmed by the current study, hydrophobic organic compounds such as fluoxetine adsorb great amounts on microplastics when in a mixture of less hydrophobic compounds. This is worrisome as a positive correlation between hydrophobicity and organic compounds toxicity has been reported (Fischer et al., 2010). The desorption of fluoxetine from PA microparticles in different media and conditions has previously been reported (Wagstaff et al., 2021). However, it has not yet been determined whether the amount of pharmaceuticals adsorbed onto microplastics are bioavailable when ingested by wildlife.

5. Conclusion

The interaction of a mixture of pharmaceuticals in contact with virgin and aged particles of six microplastic types was investigated. The properties of the pharmaceuticals, the polymer composition of the microplastics, and weathering of the microplastics were all key factors affecting the adsorption of pharmaceuticals on microplastics. Although environmentally representative concentrations were not used in this particular study, the results have clearly demonstrated the great potential of microplastics to adsorb micropollutants and potentially act as a vector in aquatic environments, especially oxidised microplastics under UV and visible light exposure. Furthermore, small particles of PP, plastic type widely used for single-use purposes and the microplastic type most commonly reported in the environment, showed to adsorb great amounts of all pharmaceuticals investigated in both, its virgin and aged state. Hydrophobic and positively charged compounds such as fluoxetine have displayed greater adsorption on microplastics when compared to hydrophilic and negatively charged compounds. It is of continued concern that pharmaceuticals adsorbed onto the microplastics can be bioavailable. However, the impact of ingested micropollutant-loaded microplastics to wildlife is yet to be determined.

CRedit authorship contribution statement

Diana S. Moura: Investigation, Visualization, Writing – original draft. **Carlos J. Pestana:** Conceptualization, Funding acquisition, Project administration, Supervision, Writing – review & editing. **Colin F. Moffat:** Resources, Supervision, Writing – review & editing. **Nikoletta Gkoulemani:** Methodology. **Jianing Hui:** Methodology. **John T. S. Irvine:** Methodology. **Linda A. Lawton:** Conceptualization, Project administration, Supervision, Writing – review & editing.

Declaration of competing interest

The authors declare that they have no known competing financial interests or personal relationships that could have appeared to influence the work reported in this paper.

Data availability

Data will be made available on request.

Acknowledgements

The authors would like to thank the Hydro Nation Scholar Programme funded by the Scottish Government through the Scottish Funding Council and managed by the Hydro Nation International Centre for funding this research. The authors would like to thank the Engineering and Physical Sciences Research Council (EPSRC) [EP/P029280/1]. In addition, the authors would like to thank Len Montgomery for proof-reading the manuscript.

Appendix A. Supplementary data

Supplementary data to this article can be found online at <https://doi.org/10.1016/j.scitotenv.2023.169467>.

References

- Akkanen, J., Kukkonen, J.V.K., 2003. Biotransformation and bioconcentration of pyrene in *Daphnia magna*. *Aquat. Toxicol.* 64, 53–61.
- Alimi, O.S., Hernandez, L.M., Tufenkji, N., 2018. Microplastics and Nanoplastics in Aquatic Environments: Aggregation, Deposition, and Enhanced Contaminant Transport. *Environ. Sci. Technol.* 52, 1704–1724. <https://doi.org/10.1021/acs.est.7b05559>.
- Almond, J., Sugumaar, P., Wenzel, M.N., Hill, G., Wallis, C., 2020. Determination of the carbonyl index of polyethylene and polypropylene using specified area under band methodology with ATR-FTIR spectroscopy. *E-Polymers* 20, 369–381. <https://doi.org/10.1515/e-poly-2020-0041>.
- Atugoda, T., Vithanage, M., Wijesekara, H., Bolan, N., Sarmah, A.K., Bank, M.S., You, S., Ok, Y.S., 2021. Interactions between microplastics, pharmaceuticals and personal care products: implications for vector transport. *Environ. Int.* <https://doi.org/10.1016/j.envint.2020.106367>.
- Bhagat, K., Barrios, A.C., Rajwade, K., Kumar, A., Oswald, J., Apul, O., Perreault, F., 2022. Aging of microplastics increases their adsorption affinity towards organic contaminants. *Chemosphere* 298, 134238. <https://doi.org/10.1016/j.chemosphere.2022.134238>.
- Boxall, A.B.A., Rudd, M.A., Brooks, B.W., Caldwell, D.J., Choi, K., Hickmann, S., Innes, E., Ostapyk, K., Staveley, J.P., Verslycke, T., Ankley, G.T., Beazley, K.F., Belanger, S.E., Berninger, J.P., Carriguirborde, P., Coors, A., DeLeo, P.C., Dyer, S.D., Ericson, J.F., Gagné, F., Giesy, J.P., Gouin, T., Hallstrom, L., Karlsson, M.V., Joakim Larsson, D.G., Lazorchak, J.M., Mastrocco, F., McLaughlin, A., McMaster, M.E., Meyerhoff, R.D., Moore, R., Parrott, J.L., Snape, J.R., Murray-Smith, R., Servos, M. R., Sibley, P.K., Straub, J.O., Szabo, N.D., Topp, E., Tetreault, G.R., Trudeau, V.L., Van Der Kraak, G., 2012. Pharmaceuticals and personal care products in the environment: what are the big questions? *Environ. Health Perspect.* 120, 1221–1229. <https://doi.org/10.1289/ehp.1104477>.
- Chamas, A., Moon, H., Zheng, J., Qiu, Y., Tabassum, T., Jang, J.H., Abu-Omar, M., Scott, S.L., Suh, S., 2020. Degradation rates of plastics in the environment. *ACS Sustain. Chem. Eng.* 8, 3494–3511. <https://doi.org/10.1021/ACSSUSCHEMENG.9B06635>.
- Chawla, K.K., 2012. *Composite Materials: Science and Engineering*, 3rd ed. Springer Verlag, New York.
- ChemAxon, 2023. Calculator Plugins Were Used for Structure Property Prediction and Calculation, Marvin 20.16.0 [WWW Document]. URL: <https://chemaxon.com/>. accessed 2.16.23.
- Chen, J., Sawyer, N., Regan, L., 2013. Protein–protein interactions: general trends in the relationship between binding affinity and interfacial buried surface area. *Protein Science: A Publication of the Protein Society* 22, 510. <https://doi.org/10.1002/PRO.2230>.
- De Bruijn, J., Busser, F., Seinen, W., Hermens, J., 1989. Determination of octanol/water partition coefficients for hydrophobic organic chemicals with the “slow-stirring” method. *Environ. Toxicol. Chem.* 8, 499–512. <https://doi.org/10.1002/etc.5620080607>.
- De Campos, A., Martins Franchetti, S.M., 2005. Biotreatment effects in films and blends of PVC/PCL previously treated with heat. *Braz. Arch. Biol. Technol.* 48, 235–243. <https://doi.org/10.1590/S1516-89132005000200010>.
- Ebele, A.J., Abou-Elwafa Abdallah, M., Harrad, S., 2017. Pharmaceuticals and personal care products (PPCPs) in the freshwater aquatic environment. *Emerging Contaminants*. <https://doi.org/10.1016/j.emcon.2016.12.004>.
- Elizalde-velázquez, A., Subbiah, S., Anderson, T.A., Green, M.J., Zhao, X., Cañas-carrell, J.E., 2020. Sorption of three common nonsteroidal anti-inflammatory drugs (NSAIDs) to microplastics. *Sci. Total Environ.* 715, 136974 <https://doi.org/10.1016/j.scitotenv.2020.136974>.
- Fan, X., Zou, Y., Geng, N., Liu, J., Hou, J., Li, D., Yang, C., Li, Y., 2021. Investigation on the adsorption and desorption behaviors of antibiotics by degradable MPs with or without UV ageing process. *J. Hazard. Mater.* 401, 123363 <https://doi.org/10.1016/j.jhazmat.2020.123363>.

- Fekadu, S., Alemayehu, E., Dewil, R., Van der Bruggen, B., 2019. Pharmaceuticals in freshwater aquatic environments: a comparison of the African and European challenge. *Sci. Total Environ.* 654, 324–337. <https://doi.org/10.1016/j.scitotenv.2018.11.072>.
- Feldman, D., 2002. Polymer weathering: photo-oxidation. *J. Polym. Environ.* 10, 163–173. <https://doi.org/10.1023/A:1021148205366>.
- Fischer, A., Hoeger, S.J., Stemmer, K., Feurstein, D.J., Knobeloch, D., Nussler, A., Dietrich, D.R., 2010. The role of organic anion transporting polypeptides (OATPs/SLCOs) in the toxicity of different microcystin congeners in vitro: a comparison of primary human hepatocytes and OATP-transfected HEK293 cells. *Toxicology and Applied Pharmacology* 245, 9–20. <https://doi.org/10.1016/j.taap.2010.02.006>.
- Gijsman, P., Meijers, G., Vitarelli, G., 1999. Comparison of the UV-degradation chemistry of polypropylene, polyethylene, polyamide 6 and polybutylene terephthalate. *Polym. Degrad. Stab.* 65, 433–441. [https://doi.org/10.1016/S0141-3910\(99\)00033-6](https://doi.org/10.1016/S0141-3910(99)00033-6).
- Guo, X., Chen, C., Wang, J., 2019. Sorption of sulfamethoxazole onto six types of microplastics. *Chemosphere* 228, 300–308. <https://doi.org/10.1016/j.chemosphere.2019.04.155>.
- He, Y., Chen, S., Zheng, Q., Chen, Y., 2014. Thermal stability and yellowing of polyamide finished with a compound anti-thermal-yellowing agent. 1263–1269. <https://doi.org/10.1080/00405000.2014.988435106>.
- Hendrickson, E., Minor, E.C., Schreiner, K., 2018. Microplastic abundance and composition in Western Lake Superior as determined via microscopy, Pyr-GC/MS, and FTIR. *Environ. Sci. Technol.* 52, 1787–1796. <https://doi.org/10.1021/acs.est.7b05829>.
- Hollande, S., Laurent, J.L., 1997. Study of discolouring change in PVC, plasticizer and plasticized PVC films. *Polym. Degrad. Stab.* 55, 141–145. [https://doi.org/10.1016/S0141-3910\(96\)00165-6](https://doi.org/10.1016/S0141-3910(96)00165-6).
- Hüffer, T., Hofmann, T., 2016. Sorption of non-polar organic compounds by micro-sized plastic particles in aqueous solution. *Environ. Pollut.* 214, 194–201. <https://doi.org/10.1016/j.envpol.2016.04.018>.
- Hüffer, T., Weniger, A.K., Hofmann, T., 2018. Sorption of organic compounds by aged polystyrene microplastic particles. *Environ. Pollut.* 236, 218–225. <https://doi.org/10.1016/j.envpol.2018.01.022>.
- Hughes, S.R., Kay, P., Brown, L.E., 2013. Global synthesis and critical evaluation of pharmaceutical data sets collected from river systems. *Environ. Sci. Technol.* 47, 661–677. <https://doi.org/10.1021/es3030148>.
- Ji Ram, V., Sethi, A., Nath, M., Pratar, R., 2019. Five-membered heterocycles. *The Chemistry of Heterocycles* 149–478. <https://doi.org/10.1016/B978-0-08-101033-4.00005-X>.
- Kandie, F.J., Krauss, M., Beckers, L.M., Masei, R., Fillinger, U., Becker, J., Liess, M., Torto, B., Brack, W., 2020. Occurrence and risk assessment of organic micropollutants in freshwater systems within the Lake Victoria south basin, Kenya. *Sci. Total Environ.* 714, 136748. <https://doi.org/10.1016/j.scitotenv.2020.136748>.
- Karlsson, T.M., Hassellöv, M., Jakubowicz, I., 2018. Influence of thermooxidative degradation on the *in situ* fate of polyethylene in temperate coastal waters. *Mar. Pollut. Bull.* 135, 187–194. <https://doi.org/10.1016/j.marpolbul.2018.07.015>.
- Koelmans, A.A., Mohamed Nor, N.H., Hermsen, E., Kooi, M., Mintenig, S.M., De France, J., 2019. Microplastics in freshwaters and drinking water: critical review and assessment of data quality. *Water Res.* 155, 410–422. <https://doi.org/10.1016/j.watres.2019.02.054>.
- Li, J., Zhang, K., Zhang, H., 2018. Adsorption of antibiotics on microplastics. *Environ. Pollut.* 237, 460–467. <https://doi.org/10.1016/j.envpol.2018.02.050>.
- Li, Y., Zhang, L., Ding, J., Liu, X., 2020. Prioritization of pharmaceuticals in water environment in China based on environmental criteria and risk analysis of top-priority pharmaceuticals. *J. Environ. Manag.* 253, 109732. <https://doi.org/10.1016/j.jenvman.2019.109732>.
- Liu, G., Zhu, Z., Yang, Y., Sun, Y., Yu, F., Ma, J., 2019. Sorption behavior and mechanism of hydrophilic organic chemicals to virgin and aged microplastics in freshwater and seawater. *Environ. Pollut.* 246, 26–33. <https://doi.org/10.1016/j.envpol.2018.11.100>.
- Liu, P., Lu, K., Li, J., Wu, X., Qian, L., Wang, M., Gao, S., 2020. Effect of aging on adsorption behavior of polystyrene microplastics for pharmaceuticals: adsorption mechanism and role of aging intermediates. *J. Hazard. Mater.* 384, 121193. <https://doi.org/10.1016/j.jhazmat.2019.121193>.
- Liu, P., Shi, Y., Wu, X., Wang, H., Huang, H., Guo, X., Gao, S., 2021. Review of the artificially-accelerated aging technology and ecological risk of microplastics. *Sci. Total Environ.* 768, 144969. <https://doi.org/10.1016/j.scitotenv.2021.144969>.
- Magadini, D.L., Goes, J.L., Ortiz, S., Lipscomb, J., Pitiranggon, M., Yan, B., 2020. Assessing the sorption of pharmaceuticals to microplastics through in-situ experiments in new York City watersheds. *Sci. Total Environ.* 729, 138766. <https://doi.org/10.1016/j.scitotenv.2020.138766>.
- Moura, D.S., Pestana, C.J., Moffat, C.F., Hui, J., Irvine, J.T.S., Edwards, C., Lawton, L.A., 2022. Adsorption of cyanotoxins on polypropylene and polyethylene terephthalate: microplastics as vector of eight microcystin analogues. *Environ. Pollut.* 303, 119135. <https://doi.org/10.1016/j.envpol.2022.119135>.
- Moura, D.S., Pestana, C.J., Moffat, C.F., Hui, J., Irvine, J.T.S., Lawton, L.A., 2023. Characterisation of microplastics is key for reliable data interpretation. *Chemosphere* 331 (138), 691. <https://doi.org/10.1016/j.chemosphere.2023.138691>.
- Mylläri, V., Ruoko, T.P., Syrjälä, S., 2015. A comparison of rheology and FTIR in the study of polypropylene and polystyrene photodegradation. *J. Appl. Polym. Sci.* 132, 1–6. <https://doi.org/10.1002/app.42246>.
- Nakatuka, Y., Yoshida, H., Fukui, K., Matuzawa, M., 2015. The effect of particle size distribution on effective zeta-potential by use of the sedimentation method. *Adv. Powder Technol.* 26, 650–656. <https://doi.org/10.1016/j.apt.2015.01.017>.
- Napper, I.E., Thompson, R.C., 2019. Marine Plastic Pollution: Other than Microplastic. Waste. Academic Press, pp. 425–442. <https://doi.org/10.1016/B978-0-12-815060-3.00022-0>.
- NCCOS, 2021. Pharmaceuticals in the Environment [WWW Document]. URL [https://products.coastalscience.noaa.gov/peiar/search.aspx](https://pro ducts.coastalscience.noaa.gov/peiar/search.aspx).
- Nurchi, V.M., Crespo-Alonso, M., Pilo, M.I., Spano, N., Sanna, G., Toniolo, R., 2019. Sorption of ofloxacin and chrysoidine by grape stalk. A representative case of biomass removal of emerging pollutants from wastewater. *Arab. J. Chem.* 12, 1141–1147. <https://doi.org/10.1016/J.ARABJC.2015.01.006>.
- Oh, S., Shin, W.S., Kim, H.T., 2016. Effects of pH, dissolved organic matter, and salinity on ibuprofen sorption on sediment. *Environ. Sci. Pollut. Res.* 23, 22882–22889. <https://doi.org/10.1007/s11356-016-7503-6>.
- Park, J., Cho, K.H., Lee, E., Lee, S., Cho, J., 2018. Sorption of pharmaceuticals to soil organic matter in a constructed wetland by electrostatic interaction. *Sci. Total Environ.* 635, 1345–1350. <https://doi.org/10.1016/J.SCITOTENV.2018.04.212>.
- Pestana, C., Moura, D.S., Capelo-Neto, J., Edwards, C., Dreisbach, D., Spengler, B., Lawton, L., 2021. Potentially poisonous plastic particles: microplastics as a vector for cyanobacterial toxins microcystin-LR and microcystin-LF. *Environmental Science & Technology* 55, 15940–15949. <https://doi.org/10.1021/acs.est.1c05796>.
- Petrie, B., Moura, D.S., Lawton, L.A., Sanganyado, E., 2023. Chiral pharmaceutical drug adsorption to natural and synthetic particulates in water and their desorption in simulated gastric fluid. *J. Hazard. Mater. Adv.* 9, 100241. <https://doi.org/10.1016/J.HAZADV.2023.100241>.
- Plastics Europe, 2021. *Plastics - the Facts 2021*.
- Prajapati, A., Narayan Vaidya, A., Kumar, A.R., 2022. Microplastic properties and their interaction with hydrophobic organic contaminants: a review. *Environ. Sci. Pollut. Res.* 29 (33), 49490–49512. <https://doi.org/10.1007/S11356-022-20723-Y>.
- Seidlitz, H.K., Thiel, S., Krins, A., Mayer, H., 2001. Solar radiation at the Earth's surface. *Comprehensive Series in Photosciences* 3, 705–738. [https://doi.org/10.1016/S1568-461X\(01\)80071-5](https://doi.org/10.1016/S1568-461X(01)80071-5).
- Seo, C., Lee, J.W., Jung, W.-K., Lee, Y.-M., Lee, S., Lee, S.G., 2022. Examination of Microcystin Adsorption by the Type of Plastic Materials Used during the Procedure of Microcystin Analysis. <https://doi.org/10.3390/toxins14090625>.
- Sharma, R., Jain, S., 2009. UV-spectrophotometric estimation of venlafaxine hydrochloride. *Asian J. Chem.* 21, 7440–7442.
- Thermo Scientific, 2007. *Calculate Reagent Log P Values to Determine Solubility Characteristics*. Thermo Scientific.
- Thompson, R.C., Swan, S.H., Moore, C.J., Vom Saal, F.S., 2009. Our plastic age. *Philosophical Transactions of the Royal Society B: Biological Sciences* 364, 1973–1976. <https://doi.org/10.1098/rstb.2009.0054>.
- Tolinski, M., 2015. Ultraviolet light protection and stabilization. *Additives for Polyolefins* 32–43. <https://doi.org/10.1016/b978-0-323-35884-2.00004-1>.
- Torres, F.G., Dioses-Salinas, D.C., Pizarro-Ortega, C.I., De-la-Torre, G.E., 2021. Sorption of chemical contaminants on degradable and non-degradable microplastics: recent progress and research trends. *Sci. Total Environ.* 757, 143875. <https://doi.org/10.1016/J.SCITOTENV.2020.143875>.
- Tourinho, P.S., Koč, V., Loureiro, S., van Gestel, C.A.M., 2019. Partitioning of chemical contaminants to microplastics: sorption mechanisms, environmental distribution and effects on toxicity and bioaccumulation. *Environ. Pollut.* <https://doi.org/10.1016/j.envpol.2019.06.030>.
- Veerasingam, S., Ranjani, M., Venkatachalapathy, R., Bagaev, A., Mukhanov, V., Litvinyuk, D., Mugilarasan, M., Gurumoorthi, K., Gunganathan, L., Aboobacker, V.M., Vethamony, P., 2021. Contributions of Fourier transform infrared spectroscopy in microplastic pollution research: a review. *Critical Reviews in Environmental Science and Technology* 51, 2681–2743. <https://doi.org/10.1080/10643389.2020.1807450>.
- Wagstaff, A., Petrie, B., 2022. Enhanced desorption of fluoxetine from polyethylene terephthalate microplastics in gastric fluid and sea water. *Environ. Chem. Lett.* 2022 (1), 1–8. <https://doi.org/10.1007/S10311-022-01405-0>.
- Wagstaff, A., Lawton, L.A., Petrie, B., 2021. Polyamide microplastics in wastewater as vectors of cationic pharmaceutical drugs. *Chemosphere* 132578. <https://doi.org/10.1016/J.CHEMOSPHERE.2021.132578>.
- Wang, Y., Yin, T., Kelly, B.C., Gin, K.Y.-H., 2019. Bioaccumulation behaviour of pharmaceuticals and personal care products in a constructed wetland. *Chemosphere* 222, 275–285. <https://doi.org/10.1016/J.CHEMOSPHERE.2019.01.116>.
- WHO, 2019. *Microplastics in drinking water*. In: *Technical Report*, pp. 1–13.
- Wu, C., Zhang, K., Huang, X., Liu, J., 2016. Sorption of pharmaceuticals and personal care products to polyethylene debris. *Environ. Sci. Pollut. Res.* 23, 8819–8826. <https://doi.org/10.1007/s11356-016-6121-7>.
- Wu, J., Xu, P., Chen, Q., Ma, D., Ge, W., Jiang, T., 2020. Effects of polymer aging on sorption of 2,20,4,40-tetrabromodiphenyl ether by polystyrene microplastics. *Chemosphere* 253, 126706. <https://doi.org/10.1016/j.chemosphere.2020.126706>.
- Wilkinson, J.L., Boxall, A.B.A., Kolpin, D.W., Leung, K.M.Y., Lai, R.W.S., Galban-Malag, C., Adell, A.D., Mondon, J., Metian, M., Marchant, R.A., Bouzas-Monroy, A., Cuni-Sanchez, A., Coors, A., Carriguiriborde, P., Rojo, M., Gordon, C., Cara, M., Moermond, M., Duarte, T., Petrosyan, V., Perikhanyan, Y., Mahon, C.S., McGurk, C. J., Hofmann, T., Kormoker, T., Iniguez, V., Guzman-otazo, J., Tavares, J.L., de Figueiredo, F.G., Razzolini, M.T.P., Dougnon, V., Gbaguidi, G., Traore, O., Blais, J. M., Kimpe, L.E., Wong, M., Wong, D., Ntchantcho, R., Pizarro, J., Ying, G.G., Chen, C.E., Paez, S., Martinez-Lara, J., Otamanga, J.P., Pote, J., Ifo, S.A., Wilson, P., Echeverria-Saenz, S., Udikovic-Kolic, N., Milakovic, M., Fatta-Kassinos, D., Ioannou-Tfoa, L., Belusova, V., Vymazal, J., Cardenas-Bustamante, M., Kassa, B.A., Garric, J., Chaumot, A., Gibba, P., Kunchulia, I., Seidensticker, S., Lyberatos, G., Halldorsson, H.P., Melling, M., Shashidhar, T., Lamba, M., Nastiti, A., Supriatin, A., Pourang, N., Abedini, A., Abdullah, O., Gharbia, S.S., Pilla, F., Chefetz, B., Topaz, T., Yao, K.M., Aubakirova, B., Beisenova, R., Olaka, L., Mulu, J.K., Chatanga, P.,

- Ntuli, V., Blama, N.T., Sherif, S., Aris, A.Z., Looi, L.J., Niang, M., Traore, S.T., Oldenkamp, R., Ogunbanwo, O., Ashfaq, M., Iqbal, M., Abdeen, Z., O'Dea, A., Morales-Saldaña, J.M., Custodio, M., 2022. Pharmaceutical pollution of the world's rivers. In: de la Cruz, H., Navarrete, I., Carvalho, F., Gogra, A.B., Koroma, B.M., Cerkvenik-Flajs, V., Gombac, M., Thwala, M., Choi, K., Kang, H. (Eds.), Proc. Natl. Acad. Sci. U. S. A., 119 Celestino, e2113947119. <https://doi.org/10.1073/pnas.2113947119>.
- Xu, B., Liu, F., Brookes, P.C., Xu, J., 2018. Microplastics play a minor role in tetracycline sorption in the presence of dissolved organic matter. Environmental pollution (Barking, Essex: 1987) 240, 87–94. <https://doi.org/10.1016/j.envpol.2018.04.113>.
- Yao, L., Hui, L., Yang, Z., Chen, X., Xiao, A., 2020. Freshwater microplastics pollution: detecting and visualizing emerging trends based on Citespace II. Chemosphere. <https://doi.org/10.1016/j.chemosphere.2019.125627>.
- Yousif, E., Haddad, R., 2013. Photodegradation and photostabilization of polymers, especially polystyrene: review. Springer Plus 2, 1–32. <https://doi.org/10.1186/2193-1801-2-398>.
- Yousif, E., Hasan, A., 2015. Photostabilization of poly(vinyl chloride) – still on the run. Journal of Taibah University for Science 9, 421–448. <https://doi.org/10.1016/j.jtusci.2014.09.007>.
- Zhang, H., Wang, J., Zhou, B., Zhou, Y., Dai, Z., Zhou, Q., Christie, P., Luo, Y., 2018. Enhanced adsorption of oxytetracycline to weathered microplastic polystyrene: kinetics, isotherms and influencing factors. Environ. Pollut. 243, 1550–1557. <https://doi.org/10.1016/j.envpol.2018.09.122>.